Meteorol. Appl. 9, 9–20 (2002)

Short-term prediction of the horizontal wind vector within a wake vortex warning system

Michael Frech, Frank Holzäpfel and Thomas Gerz
Institut für Physik der Atmosphäre, DLR Oberpfaffenhofen, D-82234 Wessling, Germany
Jens Konopka
Research and Development, DFS Deutsche Flugsicherung GmbH, D-63225 Langen, Germany

A wake vortex warning system (WVWS) has been developed for Frankfurt Airport. This airport has two parallel runways which are separated by 518 m, a distance too short to operate them independently because wake vortices may be advected to the adjacent runway. The objective of the WVWS is to enable operation with reduced separation between two aircraft approaching the parallel runways during appropriate wind conditions. The WVWS applies a statistical persistence model to predict the crosswind within a 20-minute period. One of the main problems identified in the old WVWS is discontinuity between successive forecasts. These forecast breakdowns were not acceptable to air traffic controllers. At least part of the problem was related to the fact that the forecast was solely based on the prediction of crosswind. A new method is developed on the basis of 523 days of sonic anemometer measurements at Frankfurt Airport. It is demonstrated that the prediction of the horizontal wind vector avoids these difficulties and significantly improves the system's performance.

1. Introduction

One limitation of airport capacity is caused by separation standards which were established to avoid a wake vortex (WV) hazard. First conservative separation standards were introduced in the 1970s after the B747 was launched. Extensive field programs conducted by NASA and FAA, where the wake vortex behaviour (its trajectory and evolution of strength) was measured and encounter studies were performed, resulted in different separation distances depending on the weight of the leading and following aircraft. The current ICAO separations are listed in Table 1.

In order to partially overcome this limiting factor, reduced spacing systems were designed to reduce the separation between (landing or departing) aircraft at the same level of safety. Ultimately, a reduced spacing system is thought to predict location and strength of WVs in the glide path such that the separations can be safely adjusted for departing or landing aircraft. To date none of these is operational. A summary of reduced spacing systems and research related to wake vortices can be found in Hallock *et al.* (1998).

Table 1. *Minimum required separation distances in nautical miles (nmile) between leading and following aircraft. Categories are defined according to the maximum take-off weight of the aircraft. Heavy: > 136 tons; Medium: 7 tons < weight < 136 tons; Light: < 7 tons.*

Leading aircraft	Following aircraft		
	Heavy	Medium	Light
Heavy	4	5	6
Medium	3	3	4
Light	3	3	3

The first of these systems was the Vortex Advisory System (VAS). It was designed for a single runway at Chicago O'Hare Airport. The ultimate goal of VAS was to reduce the separation standard to 3 nmile. The basic concept relies on measurements of the horizontal wind vector and detection of wake vortices indicating a reduced separation standard of 3 nmile if the wind vector is outside an ellipse with the minor axis being a crosswind of 5.5 knots and the major axis being a headwind of 12.5 knots (Hallock, 1978). This system never became operational for a number of reasons (see e.g. Hallock *et al.*, 1998).

The French wake warning system SYAGE (Système Anticipatif de Gestion des Espacements) uses wind measurements and a wake vortex model to predict reduced separations for departing aircraft (Corjon & Poinsot, 1996; LeRoux & Corjon, 1997). NASA Langely develops the Aircraft Vortex Spacing System (AVOSS) which predicts the wake vortex residence time in a control corridor along the glide path. The prediction is based on a physical wake vortex model using measured meteorological conditions (wind, temperature and TKE profile; Hinton *et al.*, 1999). AVOSS is currently designed for reducing separation standards

for single runway operations. It is planned to use a nowcasting model in the near future, which assimilates measured data in a physically based atmospheric model.

The German wake vortex warning system, WVWS, has been developed for Frankfurt Airport (Gurke & Lafferton, 1997) under contract by DFS Deutsche Flugsicherung GmbH. This airport has two parallel runways spaced 518 m apart, a distance too short for independent operations because wake vortices may be advected to the adjacent runway. Within the warning system, life times and trajectories of wake vortices are calculated. So called minimum non-hazard times for the two runways are predicted. During these periods aircraft separation can be reduced without jeopardising the existing high level of safety.

The first version of the WVWS used a persistence model to predict the crosswind within a 20-minute period. These crosswind forecasts then drive the statistical wake vortex model which is based on measurement campaigns in the 1980s at Frankfurt Airport where vortex strengths and trajectories were tracked by a LIDAR system (Köpp, 1994; Franke, 1995). This model computes vortex life time in terms of the maximum angular velocity of wake vortices and the maximum expected lateral displacement.

Meteorological conditions significantly affect life times and trajectories of wake vortices. Depending on the complexity of the warning system and the underlying wake vortex model, more or less detailed information on wind and temperature is required. Within an operational system this information is needed in real time and should allow for a forecast up to 30 minutes ahead. There are essentially two approaches to fulfil these requirements.

(a) The development of a physical model of the atmosphere and the solution of the governing equations for momentum and heat. This can be done at different levels of complexity using, for example, one-dimensional boundary layer models or sophisticated assimilation schemes to feed meteorological observations from different sources into a model to predict or diagnose the three-dimensional state of the atmosphere in the terminal area around an airport. Such systems are still under development and not yet operational (Golding, 1998; Hinton *et al.*, 1999).
(b) The use of statistical methods such as the persistence concept which assumes that the wind changes within a certain speed and angular range for the next 30 minutes. This range in wind speed and direction can either be determined from current wind measurements or it can be based on a statistical analysis of wind data taken at the same location where the forecast is needed (Gurke & Lafferton, 1997; Schlink & Tetzlaff, 1998). For the WVWS at Frankfurt the persistence concept is applied (Gurke & Lafferton, 1997). So far the glide path up to a height of 80 m is covered with the current system. This approximately corresponds to the last 1500 m of the glide path before touchdown. The extension to the entire final approach area is part of current research activities and is not the subject of this paper (see Holzäpfel *et al.* (1999) and Holzäpfel & Gerz, (1999) for first results on this subject).

In this paper we describe further developments of the wind prognosis algorithms of the German WVWS. From a careful analysis of the existing quasi-operational version we identified the crosswind prediction scheme as the main source of discontinuities in successive forecasts – so-called forecast breakdowns (FB). Quasi-operational means that the forecast product is provided to the air traffic controller who is not using the information to reduce separation of approaching aircraft. Therefore, we propose a new and improved method to predict the crosswind based on the prediction of the horizontal wind vector. The persistence concept is kept and the existing wake vortex transport and decay models are not modified in this study. The new algorithm is based on the statistical analysis of 523 days of ultra-sonic anemometer wind measurements at Frankfurt Airport.

The basic concept and problems of the crosswind forecast are discussed in sections 2 and 3. The results of the data analysis are presented in section 4. Then the new definition of wind classes is introduced (section 5). The implementation of our new forecast algorithm and the tests in an operational test environment are the subject of sections 6 and 7, where wind forecast quality and performance of the new algorithm are investigated.

2. The old crosswind forecast

The persistence model is used to predict the maximum crosswind change within a 20-minute period frame with a predefined confidence level. The forecast period is split into 2-minute timesteps. A statistical crosswind model was developed using wind measurements over a period of 134 days at Frankfurt Airport. This database was split into a 'summer' and 'winter' data sample. Classes were defined with respect to a turbulence parameter and a medium-range fluctuation parameter. The turbulence parameter is defined using the 2-minute standard deviations of the horizontal wind components. The medium-range fluctuation parameter is based on the standard deviation of ten 2-minute averages of the horizontal wind components. It provides an estimate of medium range trends in the wind field. In this way a total of 40 classes were defined. For each class and for each timestep in the forecast period an empirical probability density function (PDF) was derived from the crosswind change data sample. A 95%

confidence level was taken to determine the expected crosswind change within the forecast period.

This method of crosswind prediction is illustrated in Figure 1. At time t_0 the turbulence and medium-range fluctuation parameter are computed on the basis of current sonic anemometer measurements. These moments determine the class from which the expected maximum change in crosswind $|\Delta u_{c,1}|$ is taken. Subscript 1 denotes the maximum expected crosswind change at timestep 1 (next two minutes) within the forecast period. This crosswind change is added to and subtracted from the measured 2-minute average crosswind at time t_0. Then the predicted crosswind interval is used in the wake vortex transport model to predict the maximum horizontal displacement of the wake vortex in either direction and its lifetime for each timestep within the 20-minute forecast frame. If the horizontal displacement at a given timestep is below the critical transport distance of ±458 m, the runway is safe from wake vortices originating from the upwind runway. Note that the critical transport distance is smaller than the centre-line distance of 518 m. Here the navigational errors (2×15 m) and the location of the vortex cores off the aircraft fuselage (30 m) have been taken into account (see Gurke & Lafferton, 1997). Since the length of the predicted crosswind intervals increases with the forecast period, the outermost timestep with a lateral vortex displacement less than 458 m is defined as the maximum non-hazard time. For this period, reduced separation standards can be applied for approaches to different runways.

Four operational approach procedures are defined.

(a) *Without WVWS*. The two runways are to be used as one, because the separation standards must be obeyed (including approaches to the different runways).

(b) *Modified Staggered Approach 25L (or 25R), MSA 25L (MSA 25R)*. Wake vortices originating from aircraft landing on the downwind runway 25L (25R) do not reach the upwind runway 25R (25L). Aircraft approaching the upwind runway need to be separated from preceding aircraft landing on the downwind runway by the minimum radar separation only (2.5 nmile). Aircraft landing on the downwind runway as well as aircraft approaching the upwind runway obey the in-trail wake vortex separation standards.

(c) *Staggered Approach (SA).* Both runways can be used independently. Aircraft approaching different runways need to be separated by minimum radar separation only, whereas aircraft approaching the same runway must be separated according to the wake vortex separation standards.

(d) *Single Runway Approach (SRA).* All aircraft land on the downwind runway without considering any wake vortex separation standards. This corresponds to strong crosswinds. This approach is not implemented in the WVWS and is not part of this work.

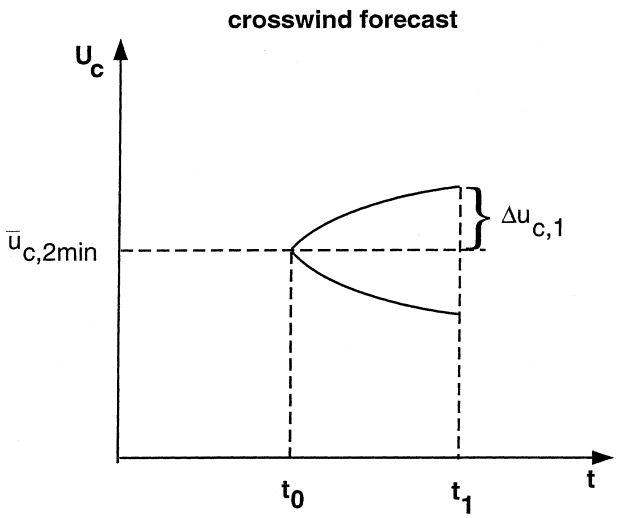

Figure 1. *Principle of the crosswind interval forecast for timestep 1. denotes the 2-minute average of the measured crosswind at time t_0, $Du_{c,1}$ denotes the expected change in crosswind at a 95% confidence level at timestep 1, t_1 = t_0+2 min.*

3. Forecast of crosswind: the problem

The system's performance has been investigated in a quasi-operational test environment. One of the problems identified were forecast breakdowns (FB). For example, a FB occurs if the system predicts a reduction of the minimum non-hazard time from 20 to 13 minutes from one timestep to the other (with a timestep of 2 minutes). That is, the minimum non-hazard time reduces faster than real time progresses. A critical forecast breakdown (CFB) is encountered if within a FB the minimum non-hazard time reduces below 6 minutes. The last 6 minutes prior to landing are important from an operational point of view since aircraft are on final approach and should be influenced by air traffic control in exceptional cases only.

The (C)FBs mean rapid changes in the predicted minimum non-hazard times, which of course, do not support staggering of the approaching traffic with reduced separation minima. CFBs result in additional workload for air traffic controllers because they have to restagger the approaching aircraft. Quantitative results of the system performance are shown in section 7 where the old and new WVWS software is tested in a quasi-operational test environment.

As we mentioned in the introduction, the forecast of the crosswind component alone is the main reason for (C)FBs. One case where this becomes apparent is the situation of a convective boundary layer. A characteristic feature of convective boundary layers are coherent structures or eddies which scale with the boundary

layer depth. Their lifetime is of the order of 5–10 minutes. These structures dominate the vertical heat and momentum transfer within the boundary layer. Under weak mean wind conditions large velocity fluctuations with no preference in direction are observed due to coherent structures (e.g. Stull, 1988). This is shown in Figure 2 where two aspects are illustrated.

(a) The convective situation in light wind conditions shows no preferred orientation of the horizontal wind vector ('sweeping wind'). Changes in u_q from 0 to 2 m s^{-1} (2 m s^{-1} is a typical velocity scale) occur on a relatively small time scale. Since the crosswind forecast is based on the measured 2-minute averaged crosswind, it is apparent that rapid changes of the crosswind can lead to FBs.
(b) The strong wind case, with a large runway parallel wind component and with small directional variation, results in the same crosswind interval as for the convective boundary layer example although we have two completely different flow situations – one with a strong variation in wind direction and the other with a weak variation. These situations could not be distinguished with the old one-dimensional consideration of crosswind only. Therefore, we propose to predict the horizontal wind vector retaining the persistence assumption.

Recently, Halsey (1998) and Schlink & Tetzlaff (1998) suggested refined versions of crosswind forecasts using an autoregressive model. They also identify the convective boundary layer conditions as one of the situations where the old forecast system fails quite often. Schlink & Tetzlaff (1998) present three cases (or rather snapshots) where their autoregressive model shows a better forecast quality than the persistence model. Whether or not this result holds under a variety of wind situations with critical wind directions is unknown.

We argue that the main problem is not the statistical method itself that is used. Prediction of the horizontal wind vector and computation of the crosswind from the predicted wind vector are expected to yield more significant improvements. Nevertheless, evaluation and implementation of an autoregressive model for the prediction of the horizontal wind vector is considered as a promising option for future work.

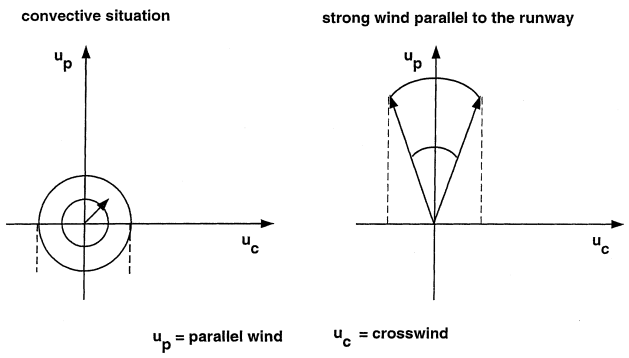

Figure 2. *Two illustrative examples which result into the same crosswind interval. The convective situation illustrates a sweeping wind with any possible wind direction, where the wind vector is assumed to fall in a ring-shaped region. The strong wind case shows a wind vector with a small directional variation.*

4. Analysis of the data

A database of 543 days of sonic anemometer data from 1995 to 1998 was available to develop the persistence forecast of the wind vector. The sonic anemometer array is located at the north-eastern end of the runway system 25 and consists of ten masts (Figure 3). The measurements are taken at 15 m height.

The data are taken with a sampling rate of 25 Hz; however, the resolution is reduced to 1 Hz for further analyses. In a first step, the quality of the data is analysed before the persistence forecast is developed. The following issues are investigated:

(a) The extent to which the database is representative in a climatological sense.
(b) The influence of different fetch conditions on the climatology: essentially there is only one direction sector from which we can expect undisturbed fetch conditions. Other directions show buildings, for example, which may disturb the wind measurements.
(c) The impact of wake vortices in the measurements on the computation of statistical moments.

The answers to these issues give an impression on the quality of the data and on the influence of ambient

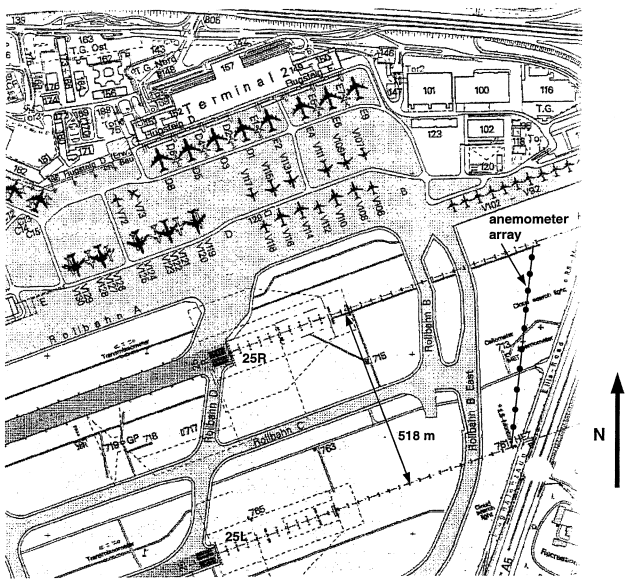

Figure 3. *The location of the sonic anemometer array at north-eastern edge of the runway. (Map reprinted with the kind permission of Flughafen Frankfurt/Main AG, FAG.)*

conditions on the wind data. The results of this analysis are used to define appropriate classes from which the statistics of wind speed and direction change are computed.

In the analysis we use the following statistical moments: to compute the average mean wind speed first, the horizontal wind components u and v are time averaged for each anemometer. Then all average components from each mast are averaged and the mean wind speed is computed as:

$$[U] = \left([u]^2 + [v]^2 \right)^{1/2}$$

The medium-range fluctuation parameter σ_U is based on the standard deviation of ten 2-minute averages of the horizontal wind components, here for mast 1:

$$\sigma_{U,1} = \left(\frac{1}{10} \sum_{i=1}^{10} \left([u_{2m,i,1}] - [u_{2m,1}] \right)^2 + \frac{1}{10} \sum_{i=1}^{10} \left([v_{2m,i,1}] - [v_{2m,1}] \right)^2 \right)^{1/2}$$

$u_{20m,1}$ and $u_{20m,i,1}$ denote the 20-minute average and 2-minute average, respectively. The average medium-range fluctuation parameter σ_U is then computed for all ten masts. Similarly, the medium-range fluctuation parameter of wind direction σ_a is computed.

In order to investigate issue (a), a climatology is derived from the WVWS wind data of 543 days. It is compared to a climatology recorded by the German weather service (Deutscher Wetterdienst, DWD). The latter climatology is based on wind data from the period 1967–97. The DWD standard weather observations and measurements are taken close to the location of the WVWS anemometer array.

The WVWS climatology shows two main wind directions, 60° and 210°, which are orographically forced. They are almost parallel to the runway orientation (70°/250°). Thus, the most difficult situation for the forecast of crosswind occurs quite frequently. Fortunately, these frequent runway parallel winds provide a broad statistical basis for development of the forecast. The comparison with the DWD climatology does not show significant differences (Figure 4) which would affect the efficiency of a forecasting algorithm in longer terms. We observe an increase of easterly winds. Moreover, the wind speed often exceeds 5 knots, when air traffic control (ATC) changes the landing direction from 250° to 70° so that the aircraft approach the airport from the south-west. Air traffic controllers confirm this observation. We conclude that the anemometer database is representative in a climatological sense for Frankfurt Airport.

To investigate the fetch conditions we define four sectors: 15°–75°, 75°–195°, 195°–255°, 255°–15°. They are chosen in such a way that the peaks of the distribution are well covered by a single interval. Moreover, changes

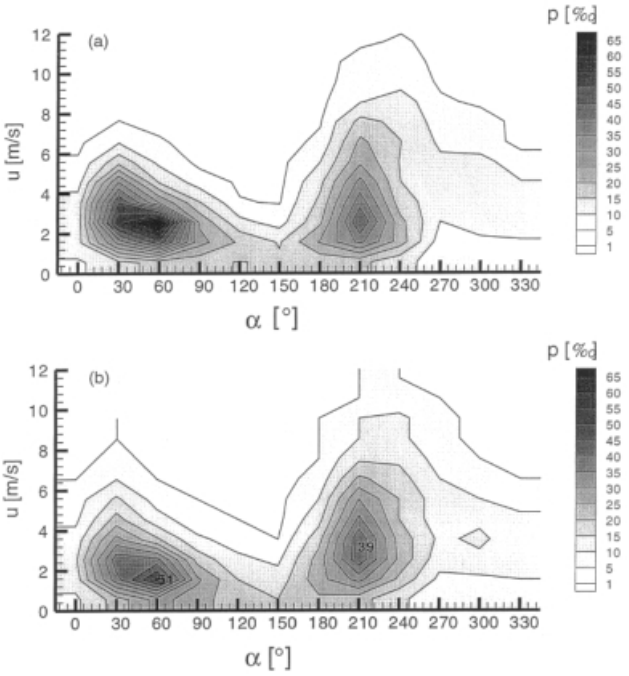

Figure 4. *The wind climatology based on (a) WVWS database of 543 days (upper panel) and (b) 30-year wind climatology recorded by the DWD (lower panel). The wind direction is given in degrees (x-axis) and the wind speed is given in m s^{-1} (y-axis). The frequency of occurrence of a certain wind speed and direction is per mill.*

from one wind class to another at a runway-parallel wind direction are avoided. In addition, the sector from 320° to 5° is defined in order to study the influence of buildings closest to the anemometer array (Figure 3). Within the sectors the medium-range fluctuation parameter is bin-wise averaged as a function of the mean horizontal wind speed. The results are presented in Figure 5.

First of all we find the typical quasi-linear increase of σ_U with increasing wind speed. In contrast, we find large σ_a values for weak wind speeds and an exponential decrease of σ_a for increasing wind speed. Thus the variability of wind direction is enhanced at lower wind speeds. Large values of σ_a correspond to the previously described convective boundary layer situation. Our analysis indicates that, in comparison to the other directions, the sector 195°–255° on average is characterised by lower σ_U values. The other sectors seem to be influenced by disturbed fetch conditions mainly due to buildings. This is especially the case for the sector 320°–5° where both σ_U and σ_a are systematically larger. An analysis of the climatological trend with respect to the influence of recent construction activities in the vicinity of the anemometer measurements indicates no systematic changes in recent years. Climatologies from different time spans (not shown here) indicate no systematic difference, for example for the northern section where buildings are located closest to the runway (about 1 km, see Figure 3).

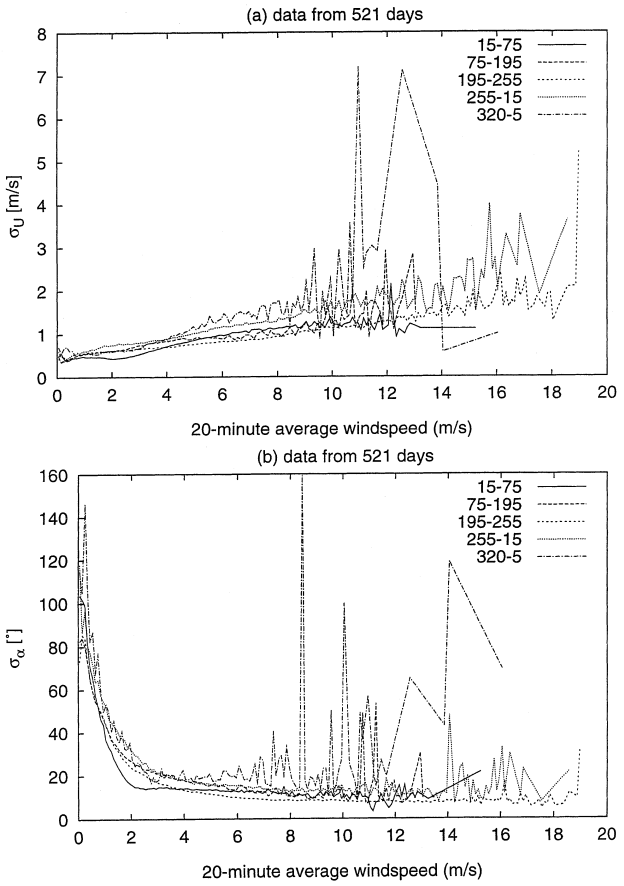

Figure 5. *(a) The bin-wise averaged medium-range fluctuation parameters (bin interval for average wind speed = 0.1 m s^{-1}) plotted versus the mean wind speed for different wind direction sectors. (b) As (a) but for α.*

The influence of wake vortices on the computation of statistical moments (i.e. mean values and standard deviations) is small. For a test case we only find a slight increase of the standard deviations due to the passage of a wake vortex through the anemometer array. The signal is more or less washed out when the average standard deviation is computed from all ten masts. We therefore see no necessity to exclude wind data which are 'contaminated' by wake vortices.

Note that the data still include synoptic scale events such as front passages which were not filtered out for our analyses. In the operational system, however, the WVWS operation with reduced separation is suspended if the DWD predicts such events for the Frankfurt Airport area.

5. Definition of classes

First, the change of wind speed and direction in a 20-minute period is computed from a database of 523 days. Anemometer measurements for 20 days are excluded in order to have a test data set against which the new forecast algorithm can be validated. These days represent different flow situations and different wind directions with respect to the runway. The computation of the expected change in wind speed and direction is illustrated in Figure 6. For each time t_0 we compute 20 ΔU and 20 $\Delta\alpha$ values within the 20-minute forecast period. At time t_0 we also compute σ_a and σ_U based on data 20 minutes before t_0. This computation requires a 40-minute data window which is translated sequentially by one-minute steps through the time series for all 523 days.

Certainly, other definitions of wind direction classes are possible. However, this choice turns out to be a good one; the relatively crude segment partitioning seems to have a rather positive impact on the system's performance. Within a direction segment we define wind speed classes characterised by 20-minute averages of wind speed and direction. The speed interval of these wind speed classes is determined by the requirement that they should contain at least 20 000 samples for each timestep within the forecast period from which the PDF of wind speed and direction change is computed. Therefore, the wind speed class width is not equidistant (see Figure 7). Each 20-minute average wind speed and direction can be assigned to a ring segment.

We showed in the previous section that there is a strong correlation between $[\overline{U}_{20\text{mins}}]$ and σ_U, and $[\bar{\alpha}_{20\text{mins}}]$ and σ_α. Therefore, we further divide the 20 000 data sample into two 10 000 data samples, which are distinguished by the medium-range fluctuation parameters.

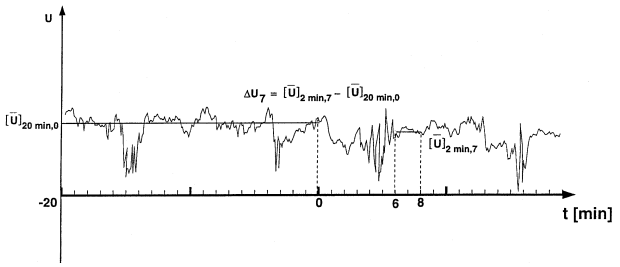

Figure 6. *Computation of wind speed change. ΔU_7 denotes the wind speed change between the 2-minute average at time t_7 and the 20-minute average*

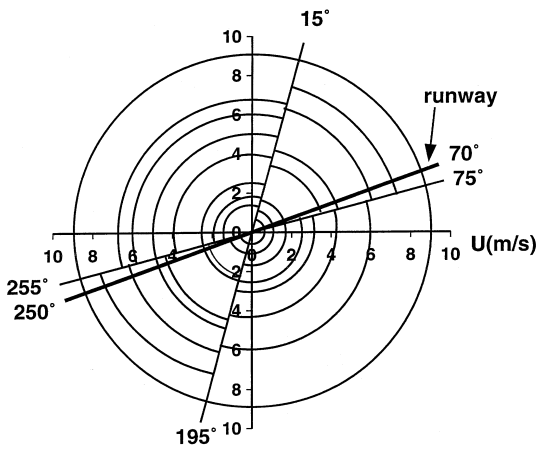

Figure 7. *Sketch to illustrate wind speed and direction classes. The orientation of the runway is also shown.*

Finally, we obtain 72 classes for which the PDFs are computed for each of the 20 timesteps within the forecast period. First, the PDFs are computed from the absolute change in wind direction and speed. Then 95% thresholds are determined from the PDF. This means that 95% of the wind speed changes (for example) fall below this threshold value within a class which is defined by the triple (U_{20m}, α_{20m}, σ_U). The corresponding triple for the wind direction changes is (U_{20m}, α_{20m}, σ_α). Because we consider wind speed and direction separately and under the assumption of no correlation between wind speed and wind direction, the forecast quality of the horizontal wind vector is expected to be not better than 95% × 95% (i.e. ≈ 90%) if we predict the wind vector using the database from which the statistics are computed.

The expected wind speed and direction change within the forecast period is shown as an example for the wind direction sector 75°–195° and the wind speed interval 0.82–1.22 m s^{-1} in Figure 8. The choice of the class depends on the value of σ_α and σ_U. The 'raw' data are plotted, based on the 95% threshold value and a fit through this data. The fit is applied in order to ensure a continuous and smooth increase of wind speed and direction change. We use this fitted data in the forecast algorithms.

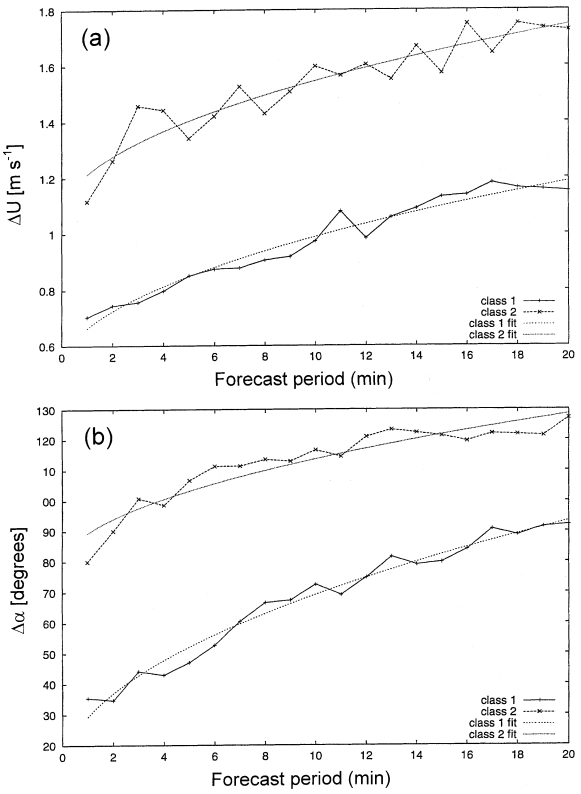

Figure 8. *(a) 95% wind speed and (b) direction change intervals within the forecast period of 20 minutes for the wind direction sector 75–195° and the wind speed interval 0.82–1.22 m s^{-1}. Plotted are the raw and fitted data for two different classes defined by σ_α and σ_U.*

6. The forecast algorithm

To obtain a forecast of the crosswind 20 minutes ahead at a given time t_0, the following steps are executed:

(a) the 20-minute averages of wind speed, direction and the medium-range fluctuation parameters are computed;
(b) these statistical moments are then used to determine the wind class;
(c) the expected maximum wind speed and direction changes are taken from this particular wind class;
(d) the crosswind is then computed from the predicted wind vector.

The 20-minute forecast period is split into one-minute timesteps. A new forecast for the next 20 minutes is computed every minute.

7. Performance and comparison to the old WVWS

The new horizontal wind forecast algorithm is tested in a quasi-operational test environment. The results are compared to the old forecast system. Before the forecast dynamics are studied, we investigate the quality of the forecast. The number of (C)FBs, critical wake vortex displacements and the total time where reduced separation standards could have been applied are analysed. The principal idea of our forecast algorithm is realised in four different versions. This variety is related to the fact that the forecast is based on discrete classes. A change from one class to another due to a sudden change in the wind vector may lead to a sudden change in wake vortex displacement which in turn can lead to a FB. This feature is inherent in this type of forecast. Depending on the resolution of the classes the change from one class to the other is more or less smooth.

The resolution is related to the size of the database from which the statistics of changes in wind speed and direction are computed. Since the size of the database is fixed in our case (523 days), we can force smooth transitions between classes applying (for example) weighted averages of the expected change in wind speed from two different classes. This may lead to improved forecast dynamics at the cost of a deteriorating forecast quality. Therefore, different approaches will be tested and compared to the old WVWS and to the new algorithm without any measures to influence the forecast dynamics (see section 7.2).

The four different algorithms are briefly introduced:

(a) *DLR pure*: the new algorithm without any additional measures to influence the forecast dynamics.
(b) *DLR MA*: unweighted moving averages (MA) of the medium-range fluctuation parameters s_U and s_a are computed, taking the current and nine previous

values. Short-term fluctuations are smoothed by this method.

(c) *DLR MA WA*: unweighted moving average (MA) of the medium-range fluctuation parameter, applied as in DLR MA but with the additional computation of a weighted average (WA) of the expected change in wind from two different s-classes.

(d) *DLR MA WA 10%*: the same method as in DLR MA WA but with a different definition of weighting factors (see Figure 9). The full maximum change of wind speed or direction z_2 is taken if $\sigma_a = \sigma_2 + 0.1\,(\sigma_3 - \sigma_2)$.

The DLR MA WA method is sketched in Figure 9.

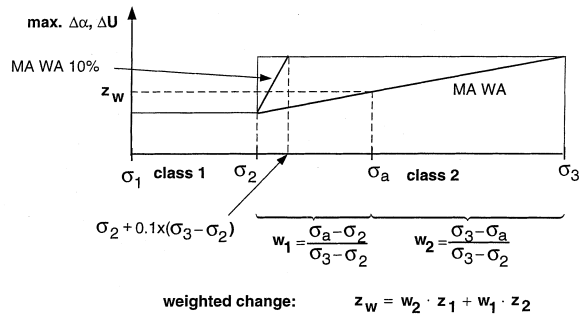

Figure 9. *The computation of a weighted average of maximum changes in wind speed and direction for an arbitrary timestep. The weighting factors w_1 and w_2 are based on the medium-range fluctuation parameter σ_a determined from the measurements. Fluctuation parameter values σ_1, σ_2, σ_3 define the class limits. In addition, the upper interval limit $s_2 + 0.1\,(\sigma_3 - \sigma_2)$ is shown, which is used in DLR MA WA 10%.*

7.1. The quality of the forecast

The different algorithms are tested against the database of 543 days and against the test database of 20 days. The results of the old algorithm are summarised in Tables 2 and 3, which show the results for every second timestep within the 20-minute forecast period.

The results are given as a percentage of the total number of forecasts of an individual forecast horizon (1–20 minutes). For example, we find that 8.76% of the predicted crosswind values are incorrect at forecast minute 10 (Table 2). Most of these incorrect crosswind values lead to incorrect wake vortex displacements (7.57%). Here, the measured crosswind at forecast minute 10, together with the wake vortex model, are used to compute the wake vortex displacement which is then compared to the predicted one. A critical displacement is given if the predicted displacement is smaller than 458 m although the displacement calculated using the real wind is larger than 458 m. A diagnosed critical displacement is not equivalent to a risk for the neighbouring runway for several reasons. The wake vortex transport model in the WVWS is very conservative in the sense that it predicts larger transport distances than observed in situ. Moreover, our analysis applies to data that are not filtered. Periods where the WVWS is not to be used to reduce separations are not excluded. For example, situations with front passages and opposite landing procedures from south-west for easterly winds stronger than 5 knots are still included in the analysis.

A detailed investigation of how often air traffic controllers need to take additional action to avoid a hazard is part of a separate safety assessment.

On average, the horizontal wind vector is within the correct limits for about 94% of the cases (Table 4) for the new algorithm 'DLR pure', which is about the same as for the old algorithm. Since we have computed the 95% values within the PDF for the change of wind speed and direction separately we first expect that the forecast quality is not better than 0.95 ? 0.95 which corresponds to 90%. That we diagnose a better quality is related to the fact that we have considered absolute changes in wind speed and direction. We carried out some tests which show slightly skewed distributions of wind speed and direction change. Of course this skewness is lost if we consider only absolute values.

Table 2. *The forecast quality of the old WVWS for 543 days.*

Measure	Forecast time (min)									
	2	4	6	8	10	12	14	16	18	20
Crosswind (%)	9.50	8.78	8.69	8.64	8.76	8.84	9.16	8.95	9.06	9.14
WV-displacement	7.89	7.44	7.46	7.46	7.57	7.68	7.96	7.79	7.88	7.96
Critical displacement 25L	0.14	0.21	0.26	0.29	0.33	0.36	0.40	0.41	0.43	0.46
Critical displacement 25R	0.12	0.20	0.23	0.26	0.29	0.31	0.33	0.33	0.34	0.35

Table 3. *The forecast quality of the old WVWS for the 20 test days.*

Measure	Forecast time (min)									
	2	4	6	8	10	12	14	16	18	20
Crosswind (%)	8.53	8.20	8.30	8.30	8.53	8.74	9.15	8.79	8.86	8.67
WV-displacement	6.97	6.90	7.02	7.17	7.36	7.59	8.04	7.78	7.86	7.58
Critical displacement 25L	0.08	0.16	0.21	0.23	0.29	0.32	0.40	0.41	0.44	0.44
Critical displacement 25R	0.12	0.18	0.24	0.24	0.24	0.27	0.25	0.21	0.19	0.18

Therefore, we achieve a more conservative prediction of wind speed and direction since we have taken absolute values of wind speed and direction change before the 95% thresholds were computed.

The number of incorrect predictions of WV-displacements is, on average, a factor of five smaller than the number of incorrect forecasts of the wind vector. The number of critical displacements is even lower. An error in the forecast of the wind vector does not necessarily lead to an error in WV-displacement. This fact is explained in Figure 10. It shows the measured wind vector at time t_0. Based on the forecast, the wind vector is expected to be within a ring segment at time t_2. From this forecast we can extract a crosswind interval $[u_1, u_2]$ which is used to compute the WV-displacement. The actual wind vector at t_2 is outside the ring segment so that we have a wind vector forecast error. However, the actual crosswind u_3 at time t_2 is still within the predicted crosswind interval $[u_1, u_2]$ so that the predicted WV-displacement is within the correct limits.

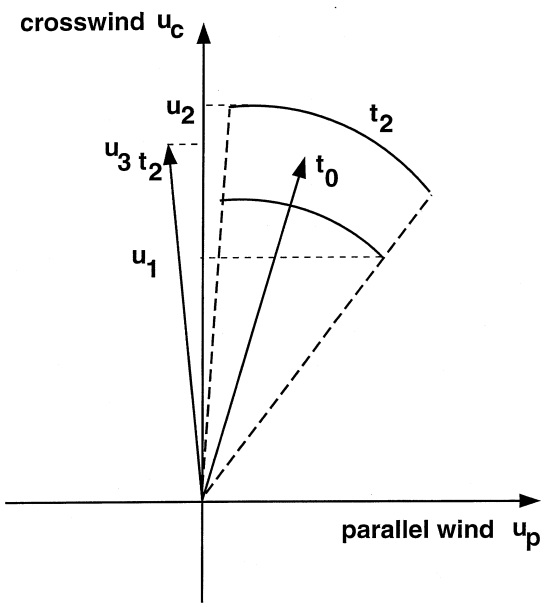

Figure 10. *Sketch to illustrate the fact that an error in the forecast of the wind vector does not necessarily lead to an error in the maximum predicted crosswind interval (see text).*

Overall, the results for the test days are again comparable to those based on the whole database (Table 5). We find a somewhat smaller number of critical WV-displacements which is probably related to the high percentage of parallel wind situations within the test database.

The results of the other algorithms are summarised in Table 6. We find the expected deterioration of the forecast quality if we apply measures to influence the forecast dynamics. However, the results of all DLR versions are still significantly better than the old algorithm. Note that with respect to the quality of the wind forecast a one-to-one comparison between the old and the new algorithms is not possible because the new algorithms predict the horizontal wind vector whereas the old algorithm predicts the crosswind component only. A comparison in terms of the WV-displacement and the critical WV-displacement is meaningful because they are directly related to the crosswind and the final minimum non-hazard time prediction.

7.2 The quality of the forecast dynamics

The forecast *dynamics* will be investigated in this section. The performance of the new algorithm is evaluated in terms of the number of C(FB)s and the possible capacity gain due to a WVWS once it is operationally used.

The main goal is a reduction in the number of (C)FBs as far as possible, with a capacity gain being of secondary importance. As mentioned in the introduction,

Table 4. *The forecast quality of the algorithm DLR pure for 543 days.*

Measure	Forecast time (min)									
	2	4	6	8	10	12	14	16	18	20
Crosswind (%)	4.69	5.66	5.92	5.78	5.68	5.94	5.98	5.86	6.05	6.39
WV-displacement	0.84	0.99	1.11	1.16	1.12	1.18	1.20	1.20	1.24	1.25
Critical displacement 25L	0.04	0.04	0.05	0.05	0.06	0.07	0.07	0.08	0.08	0.09
Critical displacement 25R	0.02	0.03	0.03	0.03	0.03	0.04	0.04	0.04	0.04	0.03

Table 5. *The forecast quality of DLR pure for the 20 test days.*

Measure	Forecast time (min)									
	2	4	6	8	10	12	14	16	18	20
Crosswind (%)	5.12	5.62	5.57	5.52	5.63	5.67	5.79	5.85	5.87	6.02
WV-displacement	0.76	0.94	1.06	1.18	1.21	1.25	1.26	1.29	1.33	1.29
Critical displacement 25L	0.02	0.03	0.03	0.02	0.03	0.03	0.04	0.04	0.05	0.07
Critical displacement 25R	0.00	0.00	0.01	0.01	0.01	0.01	0.01	0.01	0.01	0.00

Table 6. *Comparison of the different forecast algorithms. Shown is the forecast quality of each algorithm. The number of incorrect forecasts is averaged over all forecast timesteps and is given as a percentage relative to the total number of forecasts.*

Measure	DLR MA WA 10%	DLR MA WA	DLR MA	DLR pure	WVWS old
Wind	8.56	14.65	6.06	5.76	9.25
WV-displacement	1.84	3.96	1.20	1.12	7.97
Critical WV-displacement 25L	0.09	0.22	0.06	0.06	0.32
Critical WV-displacement 25R	0.05	0.14	0.03	0.03	0.27

(C)FBs are perceived by the ATC as sudden drops in the minimum non-hazard times which are visualised by coloured bars on a terminal. Recall that a reduction of the minimum non-hazard time that is larger than one minute from one timestep to the other is defined as a FB. An increase of the minimum non-hazard time is not critical. The forecast dynamics can be analysed using transition matrices. In this section we compare two examples of transition matrices (Tables 7 and 8) from two different algorithms for MSA 25R.

The first column and row in each matrix denote the predicted minimum non-hazard times of two successive forecasts, i.e. at $t = t_0$ and $t = t_0 + 2$ min. For example, let i be the index of the row, and j the index of the column (both starting with 0). The matrix element (i = 20, j = 2) equals 111 (Table 7). That is, 111 cases were diagnosed where the minimum non-hazard time changed from 20 minutes to two minutes. These 111 cases are CFBs. Ideally, the main, first upper and lower diagonal should be well filled with counts. Elements on

Table 7. *The transition matrix of the old WVWS for MSA 25R (see text for explanation).*

	0	2	4	6	8	10	12	14	16	18	20
0	155167	588	40	7	4	0	2	0	1	0	7
2	601	3648	877	215	77	33	17	26	20	5	88
4	52	812	1717	658	222	105	60	43	20	17	144
6	19	197	581	997	497	217	92	90	32	23	202
8	4	96	204	440	639	353	176	160	41	29	244
10	1	46	114	198	349	481	272	256	99	62	262
12	1	19	49	102	147	252	251	290	135	102	360
14	2	23	66	93	113	219	280	515	260	202	808
16	5	9	27	46	52	99	127	229	245	215	910
18	0	6	9	28	44	61	73	156	204	255	1181
20	22	111	143	244	280	315	359	753	864	1141	466803

(a) Minimum non-hazard time of at least 6 minutes:
percentage relative to the number of forecasts: 69.57%
(b) FB: percentage relative to (a) 5.00%
(c) CFB: percentage relative to (a): 1.45%
(d) Crit. displ.: percentage relative to (a): 0.18%

Table 8. *The transition matrix of DLR MA WA for MSA 25R (see text for explanation).*

	0	2	4	6	8	10	12	14	16	18	20
0	252817	300	99	40	18	9	5	1	3	0	10
2	318	5402	206	43	22	6	2	2	3	0	4
4	106	226	5159	231	47	14	14	11	7	1	10
6	35	43	227	4599	272	49	25	6	6	4	20
8	12	34	55	275	4001	332	46	37	9	6	73
10	4	12	10	61	302	3873	389	28	18	36	119
12	4	1	16	24	57	344	3383	406	42	9	253
14	2	1	14	8	42	53	334	2751	319	45	439
16	0	0	5	7	8	21	48	290	2597	290	448
18	0	1	2	6	5	33	9	44	253	2053	697
20	0	2	1	27	93	120	244	406	510	681	348893

(a) Minimum non-hazard time of at least 6 minutes:
percentage relative to the number of forecasts: 60.14%
(b) FB: percentage relative to (a): 2.52%
(c) CFB: percentage relative to (a): 0.35%
(d) Crit. displ.: percentage relative to (a): 0.06%

the main diagonal mean no change in the minimum non-hazard time. The first lower and upper diagonal relative to the main diagonal represent changes in the minimum non-hazard time by one minute. The fact that the other elements in the matrix are occupied by numbers larger than zero reflects the unstable forecast dynamics of the old forecast scheme (Table 7). The qualitative statement that the old algorithm shows an unstable behaviour is quantified by the analysis at the bottom of the transition matrix. In Table 7, a potential risk (d) is given if an uncritical displacement of a vortex is predicted although the observed wind conditions would suggest that a critical displacement cannot be excluded safely.

In comparison to the old algorithm, we find that the main diagonal is well occupied in DLR MA WA (Table 8). Only a relatively small number of forecasts are located on the off-diagonal elements of the transition matrix. This is also reflected by the number of FBs and CFBs, which are much smaller than for the old algorithm (FB: reduction from 5% to 2.52%, CFB: reduction from 1.45% to 0.35%). Furthermore, the critical displacements are reduced from 0.18% to 0.06%.

The results for the other algorithms are summarised in Table 9 for the three approach procedures. Except for DLR pure we find in all cases a significant improvement of the forecast dynamics for all approach procedures. At the same time the number of critical displacements is reduced by up to 90%. Note that the data have not been corrected for the periods when the WVWS will not be used because of other reasons such as thunderstorms, very poor visibility, etc.

7.3. Analysis of landing capacity

To air traffic controllers the increase in landing capacity due to a WVWS is of primary interest. The two following conditions must be met before a certain approach procedure is expected to yield a benefit in terms of capacity.

(a) The forecast must indicate a minimum non-hazard time of at least 15 minutes for at least 10 minutes.
(b) After another 6 minutes the time share for a given approach procedure is counted.

The results are summarised in Table 10. For the new algorithms the best performance is found with DLR MA WA, which is not as good as that of the old algorithm. However, it is important to remember that the forecast quality and dynamics are much better with the new algorithm. So the relatively small loss of capacity gain is more than balanced by the better forecast quality and dynamics of the new algorithm (see Tables 6 and 9). For example, the capacity gain with DLR pure is relatively small, yet it is the forecast algorithm with the best forecast quality (which determines the safety, i.e. the number of critical WV-displacements). The algorithm DLR MA WA is the best of the new algorithms with respect to capacity gain. However, the forecast quality deteriorated when measures were applied to improve the forecast dynamics. In comparison to DLR pure, these measures lead to more critical displacements while their number is still significantly smaller than that found with the old algorithm.

If we had used DLR MA WA to stagger the approaching aircraft, a reduction of separation standards would have been possible for over 80% of the time.

Table 9. *The percentages of FBs, CFBs and critical displacements of the different algorithms. The results are given for the three approach procedures and are based on the analysis of the transition matrices.*

Approach	DLR MA WA 10%	DLR MA WA	DLR MA	DLR pure	WVWS old
SA: FB	6.54	7.11	6.83	11.75	17.39
SA: CFB 1.60 1.66 3.45 6.98 5.52					
SA: Crit. WV-displacement	0.11	0.32	0.10	0.09	0.67
MSA L: FB	2.24	2.11	2.36	3.45	5.30
MSA L: CFB	0.49	0.36	0.82	1.51	1.62
MSA L: Crit. WV-displacement	0.03	0.05	0.02	0.02	0.18
MSA R: FB	3.19	2.52	3.50	5.39	5.00
MSA R: CFB	0.58	0.35	1.10	2.08	1.45
MSA R: Crit. WV-displacement	0.04	0.06	0.03	0.03	0.18

Table 10. *Time share of the different approach procedures for the tested algorithms (in %). The results are based on the analysis of 543 days.*

Approach	DLR MA WA 10%	DLR MA WA	DLR MA	DLR pure	WVWS old
SA	2.3	3.3	1.3	0.9	6.6
MSA L	39.9	42.3	35.8	34.4	42.2
MSA R	37.7	44.0	31.1	29.5	48.9

8. Conclusions

In this study we have developed a new wind forecast algorithm which predicts the horizontal wind vector in a WVWS. The persistence concept is applied. This new algorithm was implemented in a quasi-operational test environment and was compared to the old algorithm which applies a crosswind forecast. The new algorithm is based on a large database of 523 days. The wind climatology from the anemometer data was compared to a 30-year wind climatology provided by the German weather service. We show that the climatology does not appear to be influenced by the limited fetch conditions due to construction activities over recent years. However, the wind measurements indicate a higher fluctuation level for direction sectors with limited fetch conditions. The higher fluctuation level is due to factors such as buildings in the upwind area of the anemometer array which disturb the flow. Classes of wind speed and direction with respective fluctuation parameters were defined from which the maximum change of wind speed and direction was computed from probability density functions at a 95% threshold value. A total of 72 classes were defined.

The new forecast algorithm was tested against the whole database of 523 days and an independent test database of 20 days. The analysis of the forecast *quality* within the test environment shows that the forecast of the wind vector is successful. In comparison to the old algorithm the number of critical WV-displacements is significantly reduced. In order to improve the forecast *dynamics* a number of simple measures were implemented and tested. The number of FBs and CFBs is substantially reduced (by up to a factor of five).

The analysis of the landing capacity increase due to DLR MA WA indicates a moderate reduction of landing capacity in comparison to the old WVWS. But this reduction is more than balanced by the substantial improvement of forecast quality and dynamics using the new algorithm. The results show that a reduction of separation standards would have been possible for more than 80% of the time.

The new algorithm as well as the entire WVWS will be scrutinised in a separate safety assessment. The old WVWS had already improved safety compared with the single runway operated with conventional WV separation. In view of the significant improvements in comparison with the old crosswind forecast and with the very conservative wake vortex model in the WVWS, we expect a high level of safety from the new WVWS.

In a next step, DFS Deutsche Flugsicherung GmbH will extend the WVWS to cover the whole glide path. The first basic studies have already been undertaken (Holzäpfel *et al.,* 1999; 2000; Holzäpfel & Gerz, 1999; Hofbauer & Gerz, 2000; Frech & Holzäpfel, 2000) and the results will be included in the design of this new extended WVWS.

Acknowledgements

This work was funded by DFS Deutsche Flugsicherung GmbH. The comments of T. Hauf, H.-P. Schmid, R. Rudolph and the reviewers are gratefully acknowledged.

References

Corjon, A. & Poinsot, T. (1996). Vortex model to define safe aircraft separation standards. *J. Aircraft*. **33:** 547–553.

Franke, J.-M. (1995). Untersuchungen zur Dynamik von Wirbelschleppen in der atmosphärischen Grenzschicht. PhD thesis. Berichte des Instituts für Meteorologie und Klimatologie der Universität Hannover (in German).

Frech, M. & Holzäpfel, F. (2000). Sensitivity of a wake vortex model to meteorological data. In *Preprints from the EGS 25th General Assembly*, European Geophysical Society. Nice, France.

Golding, B.W. (1998). Nimrod: a system for generating automated very short range forecasts. *Meteorological Applications.* 5: 1–16.

Gurke, T. & Lafferton, H. (1997). The development of the wake vortices warning system for Frankfurt airport: Theory and implementation. *Air Traffic Control Quarterly*, **5:** 3–29.

Hallock, J. N. (1978). Vortex advisory system safety analysis, volume I: Analytical model. *Report FAA-RD-78–68*, *I* , Cambridge, MA, DOT Transportation Systems Center.

Hallock, J. N., Greene, G. C. & Burnham, D. C. (1998). Wake vortex research – a retrospective look. *Air Traffic Control Quarterly*, **6:** 161–178.

Halsey, N. (1998). The prediction of crosswind components over very short periods in the context of wake vortex avoidance. *Research Technical Report No. 244*, Met. Office, Bracknell, Berkshire, UK.

Hinton, D. A., Charnock, J. K., Bagwell, D. R. & Grigsby, D. (1999). NASA aircraft vortex spacing system development status. AIAA-99-0753, 37th AIAA Aeorospace Sciences Meeting and Exhibit, January 11–14, 1999, Reno, NV, p. 17.

Hofbauer, T. & Gerz, T. (2000). Shear-layer effects on the dynamics of a counter-rotating vortex pair. AIAA-2000–0758. 38th AIAA Aeorospace Sciences Meeting and Exhibit, January 10–13, 2000, Reno, NV, p. 7.

Holzäpfel, F. & Gerz, T. (1999). Two-dimensional wake vortex physics in the stably stratified atmosphere. *Journal of Aerospace Science and Technology.* 5: 261–270.

Holzäpfel, F., Gerz, T., Frech, M. & Dörnbrack, A. (2000). Wake Vortices in a Convective Boundary Layer and Their Influence on Following Aircraft. *Journal of Aircraft.* 37: 1001–1007.

Holzäpfel, F., Gerz, T. & Baumann, R. (2000). The turbulent decay of trailing vortex pairs in stably stratified environments. Accepted, Aerospace Science and Technology, also AIAA paper 2000–0754.

Köpp, F. (1994). Doppler lidar investigation of wake vortex transport between closely spaced parallel runways. *AIAA Journal*, **32:** 805–810.

LeRoux, C. & Corjon, A. (1997). Wake vortex advisory system implementation at Orly airport for departing aircraft. *Air Traffic Control Quarterly*, **5:** 31–48.

Schlink, U. & Tetzlaff, G. (1998). Wind speed forecasting from 1 to 30 minutes. *Theor. Appl. Climatol.* **60:** 191–198.

Stull, R. B. (1988). *An Introduction to Boundary Layer Meteorology*. Kluwer Academic, Norwell, MA.